Autoionization at the surface of neat water: Is the top layer pH neutral, basic, or acidic?

Robert Vácha,[1] Victoria Buch,[2] Anne Milet,[3] J. Paul Devlin,[4] and Pavel Jungwirth,[1*]

[1]Institute of Organic Chemistry and Biochemistry, Academy of Sciences Sciences of the Czech Republic and Center for Biomolecules and Complex Molecular Systems, 16610 Prague 6, Czech Republic, [2]Fritz Haber Institute for Molecular Dynamics, Hebrew University, Jerusalem, Israel 91904, [3]DCM UMR-5250, ICMG FR-2607, CNRS, Université Joseph Fourier, BP53, 38041 Grenoble, France, [4]Department of Chemistry, Oklahoma State University, Stillwater, Oklahoma 74078, USA

[*]Corresponding author: Pavel.Jungwirth@uochb.cas.cz

Abstract

Autoionization of water which gives rise to its pH is one of the key properties of aqueous systems. Surfaces of water and aqueous electrolytes solutions are traditionally viewed as devoid of inorganic ions, however, recent molecular simulations and spectroscopic experiments show the presence of certain ions including hydronium in the top-most layer. This raises the question about what is the pH of the surface of neat water. Microscopic simulations and measurements with atomistic resolution show that water surface is acidic due to a strong propensity of hydronium (but not of hydroxide) for the surface. In contrast, macroscopic experiments, such as zeta potential and titration measurements, indicate a negatively charged water surface interpreted in terms of preferential adsorption of OH^-. Here we review recent simulations and experiments characterizing autoionization at the surface of liquid water and ice crystals in an attempt to present and discuss in detail, if not fully resolve, this controversy.

I. Introduction

In neat water at ambient conditions one in ~$6 \cdot 10^8$ water molecules is autoionized (autolyzed), which yields the neutral value of pH = 7. Here, we assume the usual definition of pH as the negative logarithm of proton activity, which practically coincides with proton concentration at this large ion dilution. Ambient pH neutral water has equal concentrations of 10^{-7} mol/l of hydronium and hydroxide. Naively, one may attempt to extrapolate to the surface this property of bulk water. It is, however, by no means obvious, that the bulk value for the ionic product of water should also pertain for its surface.

As a matter of fact, the traditional theory of surfaces of aqueous electrolytes, based on continuum dielectric theory and point charges, views the surface as effectively devoid of ions due to image charge repulsion.[1,2] From this point of view, the question in the title of the present paper seems to be irrelevant - even if autoionization occurs at the water surface, the nascent ions should be repelled into the aqueous bulk leaving an ion-free surface layer. Recent molecular dynamics simulations, as well as surface selective spectroscopic techniques showed, however, that certain inorganic ions can be found at the aqueous surface and populations of some of them (e.g., of heavier halides) are even enhanced in the topmost layer.[3-14]

Given the above findings, the presence of the products of water autoionization at the surface cannot be *a priori* ruled out. Actually, recent molecular dynamics simulations employing different models for the hydrated proton, ranging from classical force field over an empirical valence bond scheme to density functional description, showed the occurrence and even enhancement of hydronium at the surface of water and aqueous acid solutions.[15-21] These observations are supported by

results of surface selective non-linear spectroscopic techniques, such as vibrational sum-frequency generation (VSFG)[10,14,20] and second harmonic generation (SHG),[11,13] as well as by isotope exchange IR measurements on solid aqueous nanoparticles.[21] The molecular rationalization of this effect is as follows. Hydronium with its strongly positively charged hydrogens but weakly negatively charged oxygen is a very good hydrogen bond donor but a poor acceptor. For this reason, in bulk water it tends to disrupt the local hydrogen bond network. At the surface hydronium can, however, very efficiently accommodate with an orientation with hydrogens pointing into the bulk and hydrogen bonded to neighbouring water molecules, while the oxygen sticks into the gas phase.[13,20]

In contrast, neither molecular simulations nor spectroscopic measurement indicate a strong propensity of hydroxide ions for the surface.[14,20] Although it can occasionally be found at the topmost layer, both approaches predict surface depletion of hydroxide. Unlike hydronium, OH^- with its strongly negatively charged oxygen is an excellent hydrogen bond acceptor, while the hydrogen bond donating ability of its weakly positively charged hydrogen is weaker. Therefore, while at the surface, OH^- is typically found with oxygen hydrogen bonded to neighboring water molecules and hydrogen pointing into the gas phase. However, while in the bulk, hydroxide disrupts the local water hydrogen bonding network much less than hydronium and, consequently, does not exhibit surface enhancement.[20] Thus, at the surface of neat water one can reasonably expect, based on this molecular picture, enhancement of hydronium concentration, while the corresponding enhancement of hydroxide is not anticipated. That makes a neat water surface acidic.

A different picture of enhanced surface concentration of hydroxide and depleted hydronium was proposed by colloid chemists. Surface autoionization of

water has been invoked in explaining charging effects on air bubbles and oils droplets suspended in water.[22-24] In most cases, bubbles or oil droplets in water acquire a negative charge the origin of which has been elusive. Recently, it has been suggested that this charging is due to accumulation of hydroxide anions at the air/water or oil/water interface[25-28] which seems to be in a striking disagreement with the above computational and spectroscopic results.

The principle aim of this paper is to present a detailed account of our recent *ab initio* and classical molecular dynamics simulations and IR spectroscopy, together with other calculations and measurements concerning hydronium and hydroxide at aqueous surfaces. In an attempt to address the question in the title we provide a review of arguments favoring either of the possible answers. While it is probably too early to fully resolve the existing controversy, we at least outline and discuss the possible explanations.

The rest of the paper is organized as follows: Sections II-IV provide results from calculations – classical molecular dynamics, effective valence bond schemes, and ab initio molecular dynamics. Sections V-VII summarize experimental results obtained by non-linear surface selective spectroscopies on liquid aqueous systems, low temperature surface measurements on ice nanocrystals and the amorphous solid, and zeta potential and titration experiments in aqueous systems at ambient conditions. The different approaches are compared and results are discussed in Section VIII.

II. Classical molecular dynamics simulations

The conceptually simplest computational approach with atomic resolution to surface solvation of hydronium and hydroxide is via classical molecular dynamics employing empirical force fields. The advantage of this approach is that due to its relative computational simplicity thermodynamically averaged data can be obtained for extended systems. The main drawback lies in the necessary approximations involved in the interaction potential. Since such potentials do not allow for bond breaking or making, a single canonical structure, either H_3O^+ strongly donating hydrogen bonds to three water molecules (Eigen cation) or $H_5O_2^+$ (Zundel cation) has to be assumed and no proton hopping can occur. The strong hydrogen bonding and partial charge delocalization, occurring both for aqueous hydronium and hydroxide, can be to a certain extent accounted for using a polarizable force field.

Several classical MD or Monte Carlo studies have been devoted to the study of solvation of H_3O^+ and/or OH^- in the aqueous bulk or at the air/water interface.[15,20,29-34] These studies employed simple non-polarizable or polarizable potentials for the ionic product of water, derived typically from the corresponding water potential by adding/subtracting a hydrogen atom and modifying the partial charges (and polarizabilities). A potential of mean force calculation of hydronium in a water slab showed that, unlike other small cations such as sodium, H_3O^+ is not repelled from the aqueous surface.[15] Direct MD calculations of (fully dissociated) aqueous HCl or HBr at varying concentrations employing the same potential for hydronium showed even a significant enhancement of H_3O^+ at the air/water interface.[16,20] Analogous calculations for aqueous hydroxide demonstrated that although OH^- can occasionally be found at the aqueous surface it does not exhibit surface enhancement.[20]

Recently, we have revisited the issue of surface solvation of hydroxide and hydronium with refined classical potentials and methodology.[21] We used the Gromacs molecular dynamics program package, taking advantage of its efficient implementation of the Free Energy Perturbation (FEP) method.[35] Using a recently developed automated control routine[36] we ensured that the statistical error connected with our free energy evaluations was around 1 kcal/mol.

For water a polarizable POL3 model was employed.[37] For H_3O^+ and OH^- we started with a simple polarizable force field, which we used previously.[20] For the Zundel ion $H_5O_2^+$ Lennard-Jones parameters were taken from the POL3 water and charges were calculated by the RESP method based on a B3LYP/cc-pvtz calculation.[38]

The force field of H_3O^+ was then modified by adjusting the Lennard-Jones parameter σ on oxygen to fit ab initio MP2/aug-cc-pvdz interaction energies of hydronium with the three most strongly bound water molecules. Additionally, we aimed at fitting the B3LYP/DZVP energy differences between structures with proton inside or at the surface of a cluster containing 48 water molecules *(vide infra)*. To remain within physically reasonable values, the fitted σ parameter was modified only within 10 % of its original value. This allowed us to match closely the ab initio binding energy of the strongly bound three water molecules. The B3LYP energy preference of surface structures of the $H^+(H_2O)_{48}$ was reproduced qualitatively by our best empirical potential but quantitatively remained somewhat underestimated. It is thus reasonable to assume that our classical MD simulations provide a lower bound to the surface enhancement effect of hydronium. The optimal sets of force field parameters for H_3O^+, $H_5O_2^+$, and OH^- are presented in Table 1.

Our extended system consisted of 432 water molecules placed in a rectangular

cell with dimensions of 18.7 Å, 18.7 Å, and 237 Å which yielded after application of periodic boundary conditions an infinite slab of a 40 Å thickness in the z-direction. Either a single ion (H_3O^+, $H_5O_2^+$, or OH^-), or both cation and anion were added to the slab. The resulting free energy difference between a surface and bulk position of each of the ions was practically uninfluenced by the presence of the counterion in the slab. Figure 1 depicts a characteristic snapshot of the corresponding water slab with a single hydronium at the surface and hydroxide ion in the bulk. Nanosecond time-scale simulations were performed employing a 1 fs time step. An interaction cutoff of 9 Å was employed. The effect of long-range Coulomb interactions was treated by the Particle Mesh Ewald (PME) method.[39] The system was simulated in the NVT ensemble with temperature held at 300 K. Intramolecular O-H bonds were kept rigid at their optimal values.

All tested models of H_3O^+ (as well as the $H_5O_2^+$ Zundel ion) showed preference for the air/water interface. The parametrization of H_3O^+ which was in best agreement with ab initio data favored surface by ΔG = -3 kcal/mol, which corresponds to a ~150 times enhanced surface concentration of hydronium compared to bulk. This enhancement can be translated to surface pH of ~4.8 assuming an activity coefficient of unity. Namely, pH is given as the negative logarithm of H_3O^+ surface concentration, which is that of the bulk neat water multiplied by a Boltzmann factor of $\exp(-\Delta G /RT)$ at T = 300 K. Since our parametrization underestimates the surface preference of hydronium in clusters of 48 water molecules by about 4 kcal/mol compared to B3LYP values, the above pH value is likely to represent an upper bound (assuming an additional ~4 kcal/mol surface preference as suggested by the DFT cluster calculations discussed below would lower the surface pH to about 1.9). In contrast, for OH^- we observed a weak preference for the bulk of 1 - 2 kcal/mol, which can be translated to

pOH in the range of 7.7 - 8.4.

III. Effective valence bond and proton hopping schemes

The classical force field outlined in the previous section does not allow for making and breaking of chemical bonds; therefore, proton hopping in water cannot be described within its realm. Several molecular dynamics schemes exist which account for proton hopping and still essentially remain within computationally efficient classical molecular dynamics. These are in particular the Empirical Valence Bond (EVB) approach[16,40] and the stochastic proton hopping Q-HOP method.[41]

The multistate EVB method has been applied to investigate the behavior of a single proton both in water clusters[42,43] and in an aqueous slab.[16] These calculations revealed a strong propensity of hydronium for the liquid surface, be it that of a finite size cluster or extended slab. Similarly, the Q-HOP approach (which did not include polarization interactions) showed that hydronium is not repelled from the surface of a water slab (unlike other cations such as, e.g., sodium).[20]

IV. Ab initio studies: minimizations and molecular dynamics

Water clusters and liquid slabs

An indication that a proton in water may prefer surface positions came also from ab initio studies of protonated clusters.[17-19] Specifically, the $(H_2O)_{21}H^+$ cluster was investigated by ab initio minimizations,[17-18] and by ab initio molecular dynamics.[19]

Structures with proton in the interior were less favorable by ~10 kcal/mol than those with a surface proton location. Nevertheless, the applicability of these results obtained for a medium sized cluster of a specific geometry to larger clusters and to the liquid is not straightforward. This issue is further pursued below.

In the present study, two routes of *ab initio* research were taken to further clarify the issue. First, NVT *ab initio* molecular dynamics simulations were carried out for liquid water with either an H_3O^+ or OH^- ion, and with both ions present. To elucidate surface effects, simulations were done both for a cubic box with three-dimensional periodic boundaries and for a slab with two open surfaces and two-dimensional periodic boundaries. This "on-the-fly" technique enables first-principle modeling of proton transfer systems at finite temperatures; proton transfer and transitions between the different protonated water forms – Zundel and hydronium, are automatically included in the computational scheme. However the high computational cost limits the dimensionality of the model system, the duration of the trajectories, and the accuracy of the electronic structure method used to evaluate the forces and the energies. Direct simulation of autoionization is not easily feasible due to the activation barrier (see however a pioneering study of bulk autoionization in Ref. 45). On the other hand, recombination between H_3O^+ and OH^- can be readily observed in on-the-fly simulations, on a accesible time scale, enabling qualitative assessment of the autoionization energetics.

On-the-fly results suggest significant lowering of endothermicity of the autoiozation reaction at the surface, with respect to the bulk, due to stabilization of hydronium at the interface.[21] To assess quantitatively the extent of this stabilization, *ab initio* techniques were then applied to calculate the energy of a protonated water cluster

$(H_2O)_{48}H^+$ with the proton either at the surface or in the interior. At this size, fairly accurate electronic structure calculations can be made for the system energetics. A similar study was carried out for $(H_2O)_{47}OH^-$.

Ab initio molecular dynamics: Methods and results

The *ab initio* molecular dynamics simulations employed the on-the-fly NVT code as implemented in the CP2K/QUICKSTEP package.[45] The scheme combines a Gaussian basis for the wave functions with an auxiliary plane wave basis set for the density. The DFT/BLYP method was employed in conjunction with the DZVP basis, and pseudopotentials of the Goedecker-Teter-Hutter type.[46] The time step was 0.5 femtosecond. The first simulation pertained to a slab of 72 water molecules in a 13.47 × 15.56 Å two-dimensional periodic box; the thickness of the slab was ~11 Å. Such a slab has a well defined surface and subsurface region, although the bulk part is somewhat too small.[47] Martyna-Tuckerman Poisson solver was used in the calculations with 2D periodic boundaries.[48] In simulations with a single ion, one of the surface water molecules was converted initially to either H_3O^+ or OH^- by addition or subtraction of H^+. Additional simulations were carried out for a zwitterionic system, after converting two water molecules to H_3O^+ and OH^-. The second set of simulations pertained to 64 water molecules in a cubic box of dimension 12.41 Å, with 3D periodic boundaries. For the above computational parameters, the water self-diffusion constant in a 3D box is 2.50 and 0.52 10^{-5} cm^2s^{-1} at 300 and 270 K, as compared to the experimental values of 2.57 and 1.13 10^{-5} cm^2s^{-1} at 298 and 273 K, respectively.[50,51] The simulations were carried out finally at 270 K, since at this temperature it was easier to stabilize the hydronium-hydroxide ion pair within the finite size box.

First, a single ion (H_3O^+ or OH^-) was simulated in an 11 angstrom thick water slab containing 71 water molecules. Throughout a 2.5 picosecond (ps) simulation, the cation remained at the surface. In a similar simulation, the anion underwent initially

several quick proton transfer cycles between the surface and the interior, but after 0.3 ps settled in the interior of the slab for the remainder of the simulation.

Simulation of a slab including both of the ions (H_3O^+ and OH^-) required some effort, since, due to the limited dimensionality of the model, the ions tended to recombine before relaxing. Different initial locations were tried for the two ions. Finally, a trajectory was generated in which the two ions acquired favorable solvation shells prior to recombining and thus survived for the duration of 5.4 ps. During the first picosecond of this trajectory, the two ions formed an interesting solvent-separated ion-pair, with the central water molecule acting as proton acceptor with respect to both ions. In this configuration, recombination is blocked by the central water molecule - such configurations may in fact serve as intermediates in the autoionization process in water. (See discussion in Ref. 44 concerning the need to break the proton wire in order to stabilize a newly formed ion pair.) During this first part of the trajectory, the ion pair resided in the slab interior; however the proton underwent numerous back-and-forth transitions between the ion-pair configuration and the surface. At t ~ 1 ps, the two ions separated; proton moved to the surface, while hydroxide adopted an interior position. The ions remained so until just before recombination (t ~ 5.3 ps), at which time the anion emerged at the surface.

Figure 2A shows the energy of the system along this trajectory, together with the energy profile for a trajectory of a neutral water slab without the ions. The two energies are the same within the accuracy of the calculation. The energy difference between the autoionized and neutral system cannot be assessed quantitatively from this calculation, both due to the limited accuracy of the DFT/BLYP method and because of the large potential energy fluctuations of the finite dimensionality systems. However one may note the qualitative difference with respect to an on-the-fly simulation of the corresponding bulk system, employing cubic three-dimensional periodic boundary conditions, for which the energy of the autoionized system clearly exceeded the energy

of the neutral one. (Fig. 2B). Note also that in Fig. 2B the drop in potential energy is delayed by 1 ps with respect to recombination (marked by the arrow) since the surrounding water molecules need some time to relax to the new environment of the recombined ion pair.

The calculated mean energy differences between the Zwitterionic and neutral systems are -2 ± 18 kcal/mol, and 31 ± 16 kcal/mol, for panels (A), and (B), respectively. While the error bars are large, the above on-the-fly results are consistent with preference of protonated water for surface sites, and suggest reduced endothermicity of autoionization at the liquid surface due to surface stabilization of the cation.

Search for low energy structures of $(H_2O)_{48}H^+$ and $(H_2O)_{47}OH^-$ clusters

The crucial quantity for the present argument is thus the free energy lowering as the proton is moved from the aqueous bulk to the surface. The main contribution is expected to originate from the energy change due to surface stabilization of the proton. An effort is now made to obtain a reasonably accurate estimate of this energy change. The model used in this part is a protonated water cluster $(H_2O)_{48}H^+$, with the proton either on the surface or in the interior. At this size, B3LYP calculations can be made of the system energetics. B3LYP method is expected to yield much more accurate energy values than BLYP used in the slab calculations; as a matter of fact, this method benchmarked very well against more accurate MP2 and CCSD(T) calculations for autoionization in the water octamer.[51]

Past studies showed that low energy structures of the neutral analog $(H_2O)_{48}$ can be described as compact 3D amorphous;[52] these structures display excess of under-coordinated surface molecules with respect to clusters of larger sizes. Thus, the present cluster size may not still approach the bulk behavior,[52] but it is the largest we could

tackle effectively and accurately with our computational means, exploring a large number of possible minima (*vide infra*). Nevertheless, the amorphous cluster structure appears to be a reasonable model for molecular arrangements at the liquid surface. Moreover ice nanocrystals, which are the topic of the experimental study described below, were shown in the past to have crystal interiors and a non-crystalline surface layer.[52] Thus the present cluster model can also approximate reasonably the behavior of ice nanocrystal surfaces and subsurfaces.

A pre-search for possible low energy structures of $(H_2O)_{48}H^+$ employed a classical molecular dynamics-based method described in Ref. 53. NVE trajectories lasting several nanoseconds were run for the cluster at a mean temperature ~200 K. At this stage, the calculation employed a non-polarizable empirical potential for the hydronium-water system (standard TIP4P water model[54] and hydronium with polarizability turned off) in order to speed up the pre-search of possible configuration. Trajectory structures were minimized every 5 ps. A bank of ~1200 potential minima was thus obtained, with hydronium either at the cluster surface, or in the interior. The energies of the minima were then recalculated at the BLYP/DZVP level, following a single minimization step. Ten thus-obtained lowest-energy structures of each kind were subjected to full minimization at the BLYP/DZVP level. The final energies were recalculated at the B3LYP level. The average energy difference between 10 lowest energy minima with the proton in the interior and 10 lowest energy minima with the proton at the surface was 8.7 kcal/mol and 10.5 kcal/mol, for B3LYP and BLYP, respectively, in favor of surface structures. Three of the lowest energy minima of each kind were furthermore fully reoptimized at the B3LYP level; resulting in a 8.8 kcal/mol energy difference between a pair of lowest energy minima of each kind. As noted above, this energy preference for surface structures is consistent with values obtained by other authors for smaller $(H2O)_{n=20,21}H^+$ clusters[17-19] which, however, acquire a rather special cage-like geometry.

Similar studies were carried out for the $(H_2O)_{47}OH^-$ cluster. A set of 800 structures, each with OH^- either at the surface or in the interior of the cluster were first generated by classical molecular dynamics runs. Then, energy was recalculated, after a single minimization step, with QUICKSTEP, at the BLYP/DZVP level. One may note at this point that there has been a considerable controversy over the coordination number of the hydroxide ion in water, which was shown to depend on the electronic structure method used (see Ref. 55, and references therein). According to on-the-fly results,[55] the BLYP functional is a realistic choice, yielding a physically reasonable diffusion constant and mechanism; the typical bulk coordination with respect to water corresponds to 4 acceptor bonds and one transient donor bond. The simple empirical potential used to construct the initial set of configurations favors a somewhat higher coordination, nevertheless, the set included configurations for a range of hydroxide coordinations. The following structures were then subjected to the full BLYP/DZVP level minimization yielding (a) five lowest energy structures with OH^- in the interior, five acceptor bonds and a weak donor bond, (b) five lowest energy structures with OH^- in the interior, four acceptor bonds and a weak donor bond, and (c) five lowest energy structures with external OH^-. For all thus minimized structures, a single point calculation of the energy was carried out at the B3LYP/6-31+G** level (a set of diffuse functions was added because of the anionic character of the cluster).

Interestingly, at the BLYP/DZVP level, structures of group (a) were found to be favored energetically with respect to group (b); the average energy of group (a) being lower by 3.6 kcal/mol than the that of group (b). Similarly, the energy of the "best" five acceptor bonded structures with OH^- in the interior was lower by 2.6 kcal/mol than that of the best four acceptor bonded structures. Interestingly, at the more accurate B3LYP

level,[51] the difference between the average energies of the two groups of structures with interior hydroxide almost disappeared (being reduced from 3.6 kcal/mol to only 1.0 kcal/mol). Moreover with B3LYP, the most favorable four acceptor bonded structure had a slightly lower energy (by 0.04 kcal/mol) than the most favorable five donor bonded structure.

Finally, the five lowest energy structures at the B3LYP level with OH^- in the interior included two four coordinated and three five coordinated structures. Among the five lowest energy structures with OH^- at the surface (also at the B3LYP level), the most favorable one corresponded to 3 acceptor bonds, whereas the rest corresponded to 4 acceptor bonds. The hydrogen of hydroxide was uncoordinated and pointed out of the cluster. Comparing average energies of the five best internal vs five best surface structures of hydroxide in the $(H_2O)_{48}$ cluster gives a preference of 5.4 kcal/mol for interior solvation of OH^-. The energy of the best interior hydroxide structure found is lower by 2.9 kcal/mol than that of the best surface structure.

Crystalline ice slabs

A set of investigations was carried out also for hydronium and hydroxide ions in/on a perfect ice crystal slab, containing three hexagonal (basal plane) bilayers, with 24 water molecules each. Perfect crystal surfaces are very difficult to prepare[56,57] and it is possible that under "normal" conditions the top ice bilyer(s) are disordered. Nevertheless, the behavior of ions under idealized crystal conditions is also of interest. Our studies focused on minimization and molecular dynamics runs of ice structures with either of the ions or both present, using QUICKSTEP on the BLYP/DZVP level, with 2D periodic boundaries.

It should be noted that ice is an orientationally disordered solid. Only oxygen atoms form a periodic pattern, while the water orientations are random within the constraints of completeness of the H-bond network.[58,59] Hexagonal ice bilayers are puckered. In the surface ice bilayer, the "upper" half of molecules is three-coordinated, with either a dangling-H (d-H) or dangling-O (d-O) atom, and the lower half is 4-coordinated (see Fig. 3). While for the bulk the different orientational arrangements are nearly isoenergetic,[58-60] a much broader span of energies is obtained at the surface.[61-62] This is since various orientational arrangements result in different patterns of surface dangling atoms which interact with each other strongly via partial charges. In particular, presence of clumps of dangling-H atoms (which stick out of the surface) raises the energy substantially.

Models with hydronium or hydroxide were conveniently generated by adding an H-atom to a d-O surface molecule, or removing H from a d-H molecule. These initial configurations are unstable. However in the course of the ensuing structure minimization, a sequence of barrierless proton-transfer transitions occurred, which resulted in stable ion configurations such as the ones shown in Fig. 3A, with the ions occupying one of the three-coordinated lattice sites in the upper half of the surface bilayer. In these configurations, the hydronium ion forms three proton donor bonds, while the hydroxide ion forms three proton acceptor bonds; see Fig. 3B. Numerical experiments show that the ion energy depends also on the pattern of dangling atoms in the surrounding second near-neighbor positions (marked by circles in Fig. 3). The most favorable pattern is symmetric, with alternating d-O and d-H.

One striking result is the observation of barrierless long range proton transfer transitions along proton wires, during the minimizations, as in Fig. 4. Here, a

hydronium and hydroxide ion pair was generated initially at a second nearest neighbor positions. Since the ions were separated by a double-donor water molecule, direct recombination was not possible. Recombination did occur in this particular run at the 97th step of the minimization, following several proton-jump events by each ion. Note that the sizable energy drop occurred largely during relaxation after recombination, similarly to liquid water calculations described above.

Zwitterionic systems which are stable with respect to minimization could be generated by placing the two ions at the two sides of the slab. The most stable zwitterionic system found, with energetically favorable ion and dangling atom configurations, had energy 9 kcal/mol above the neutral slab with energetically favorable dangling atom configuration. (This result is qualitative since thermal averaging over possible orientational configurations was not carried out yet.)

One of such stable zwitterionic systems was used as an input for a MD simulation. At ~70 K the ions did not move, while at ~210 K recombination occurred at a very short timescale of 1 ps, following a complex sequence of proton transfer events within the surface and across the slab.

V. Non-linear surface selective spectroscopy

Non-linear (three-photon) spectroscopic techniques such as VSFG and SHG are well suited for studying solutes at aqueous interfaces since their signal vanishes in the bulk region. However, these spectroscopies do not probe only the top-most layer of the liquid but the whole interfacial layer with lack of inversion symmetry. In neat water[63,64]

it is estimated that the signal comes dominantly from about 2-3 molecular layers with the contribution from the top-most layer being most important.

The concentration of hydronium or hydroxide ions in neat water is unfortunately too small to provide a measurable signal in these non-linear spectroscopies. Therefore, the surface propensity of these ions was investigated in aqueous solutions of strong acids (e.g., HCl, HBr, or HI) or bases (NaOH) at varying concentrations.[10,13,14,20] Presence of a strong acid has a dramatic effect on the VSFG spectra, both in *ssp* and *ppp* polarizations, probing predominantly vibrations perpendicular and parallel to the surface. The strong increase in intensity in the hydrogen-bonded OH stretch region (3200 – 3400 cm^{-1}) and slight decrease in the free OH region (3700 cm^{-1}) is readily interpreted in terms of the presence and enhancement of hydronium cations in the interface layer including the top-most layer.[20,22] In contrast, no such effect has been observed for hydroxide anions. The VSFG spectra of aqueous NaOH do not differ appreciably from those of neat water. More precisely, a small decrease in intensity in the hydrogen bonded region is observed in *ssp* polarization and virtually no effect in *ppp* polarization, which is interpreted in terms of a lack of significant activity of OH^- in the interface, particularly in the top-most layer.[14,20]

SHG results support the above conclusion from VSFG measurements concerning surface activity of hydronium.[13] The SHG techniques is presently not capable of directly probing H_3O^+ but it can compare the signal from the halide counter-anion for an acid to that for the corresponding salt solution. Comparison of SHG spectra of iodide in aqueous HI vs NaI shows a significant increase in intensity upon moving from the salt to the acid. This is interpreted in terms of surface active hydronium cations which help to "drag" additional iodide anions into the interface by Coulomb forces.[13]

VI. Surface experiments at low temperatures

Experiments on Solid Water with Emphasis on the Water-Ambient Interface

Experiments designed to reflect proton behaviour on the surface of ice have multiplied greatly in the past two decades stimulated partly by the recognition of a likely role in stratospheric chemistry of particles of the Antarctic fog, within the winter polar vortex, leading to ozone depletion. Most such studies, which have emphasized the behaviour of HX (X = Cl, Br) and HNO_3 at dosage levels of monolayer coverage or greater, are not examined in detail in this section. Rather, the emphasis is on bare ice, either crystalline or amorphous, with results invoked from small surface dosage with acids and bases where they are informative of proton or hydroxide ion activity at or near the ice surface.

Historically, proton activity in ice was investigated extensively using conductivity and dielectric relaxation measurement.[58] Unfortunately, useful conductivity measurements were difficult for pure ice, with many results later proven unreliable because of surface contributions of unknown magnitude. These types of studies became rare following the careful analysis of dielectric data[65] which led to the conclusion that protons probably do not conduct charge within bulk ice. This and more recent studies of charge transport within ice, primarily by the group of Petrenko, have been thoroughly reviewed in a book on ice physics.[59]

Studies of proton transport in ice using molecular-level probes were initiated during the 1980's.[66,67] It was shown that isotopic exchange within ice, prepared with non-equilibrium mixtures of H_2O, D_2O and HDO, could be followed quantitatively with FTIR difference methods. Based on the generally accepted concept that isotopic scrambling within ice at low temperatures requires a combination of proton hopping and molecular turn steps (the latter promoted by mobile orientational defects) the studies

appeared to show conclusively that protons do move within ice at temperatures as low as 130 K. For example, intact isolated D_2O molecules within thick films of polycrystalline H_2O ice (~3 microns) were converted to isolated HDO molecules on time scales ranging from 3 hours at 135 K to a few minutes at 150 K. Isotopic exchange experiments also showed that non-thermal creation of protons, through visible photon excitation of overtone vibrations, leads to proton activity at substantially lower temperatures.[68]

More recent conclusions, based on the behaviour of soft-landed protons on thin ice films, once again challenged the concept of mobile protons in ice and have been used, in particular, to argue against proton transfer beyond near-neighbour distances.[69] However, following that study, it was demonstrated, via the FTIR isotopic-exchange approach, that proton activity throughout ice nanocrystals is enhanced by adsorbed HCl.[70] Further, Kang et al. then showed, via reflective ion scatter (RIS) from the surface of an amorphous ice film, that D_2O and H_2O alternating ultra-thin films participate in proton transfer. However, the latter evidence was convincing only for the surface and perhaps one or two subsurface layers of amorphous ice.[71,72]

This review section focuses on the nature, results and interpretation of the study of proton activity (a product of concentration and average mobility) within and on the surface of ice using molecular probes: FTIR monitoring of exchange by D_2O isolated in H_2O nanocrystals, reflective ion scattering from H_2O – D_2O films, and surface soft-landing of protons. Particular emphasis is be given to two most recent studies; the RIS thin-film work of Kang et al.[73] and our current results for ice nanocrystals.[21] Both of these studies offer additional strong evidence of the ability of protons to move within ice, while also indicating an at least order-of-magnitude greater proton activity at the ice surface relative to the interior. The new ice nano-crystal data also confirm an ability to control the interior proton activity through surface exposure to acid and base adsorbates.

Two basic approaches have emerged for preparation of samples for the study of proton-induced H-D isotopic exchange. Either the D_2O probe molecules are isolated at substitutional sites within H_2O ice, or D_2O exposure to H_2O ice is provided at the interfaces of alternating D_2O and H_2O thin layers. The FTIR spectroscopic studies of proton activity, whether of thick-film deposits or of ice nanocrystals, have used H_2O ice containing isolated substitutional D_2O molecules. By contrast, RIS studies of proton activity have depended primarily on isotopic exchange involving H_2O and D_2O molecules separately deposited within ultra-thin layers.

Exchange of Isolated D_2O in Ice Films and Nanocrystals

The functioning of point defects in H_2O ice, with conversion of isolated D_2O to isolated HDO, can be understood from the diagrams of Fig. 5. A small section of crystalline ice is represented in the top panel, with the orientational L (Bjerrum) defect depicted at the left and the proton defect shown as the hydronium ion on the right. This concentration of defects is not realistic, since the molarities in pure ice are not expected to exceed 10^{-8} at the relevant temperatures. Both types of defects occur as pairs (L, D and H^+, OH^-) within separate dynamic equilibria, but the emphasis is normally on the L and H^+ defects because the D and OH^- are relatively immobile.[74] Modern structural representations of the Bjerrum L and D defects[75] and of the hydronium ion in ice[76] are available.

Two steps in the isotopic-exchange sequence are represented in the bottom two panels of Fig. 5. The middle panel shows the conversion of D_2O, to a neighbour pair of tandem HDO molecules, by the passage of a hopping proton. However, the hop-step can do no more than move a deuteron back-and-forth within a hydrogen bond, so a different type of defect action is needed for further separation of the deuterium atoms. Passage of the L defect (turn step, bottom panel) provides this next step towards isolated HDO molecules. Because the isolated D_2O, the tandem HDO pair, and the isolated HDO each

have unique infrared O-D stretch bands,[67,77] the relative amount of the three different D isotopomers can be determined from FTIR spectra at any stage of the exchange process; so proton activity can be monitored quantitatively.

Though the loss of isolated D_2O may initially follow first order kinetics, the reversibility of the exchange steps quickly leads to more complex kinetics; so it is necessary to include at least one additional exchange step (beyond the 2 steps of Fig. 5) in the analysis.[66] Published kinetic results include isolated D_2O half-lives for temperatures ranging from 135 to 150 K, with activation energy for proton activity of 9.5 kcal/mol. Most simply, this energy can be assigned to a combination of the formation and mobilization energies of the proton,[58] but there is considerable evidence that the shallow trapping of protons, perhaps by L defects, contributes to this activation energy.[67,69,78]

The sequence of Fig. 5, and the associated spectroscopy and exchange kinetics applies to the interior crystalline ice of both thick films and nanocrystals. The interior proton activity is similar, whereas the L-defect activity is an order of magnitude greater for the nanocrystals with the nearby surface apparently serving as an L-defect source.[70] The structural situation is much different for the ice surface for which the molecules in the outermost layer are three-coordinated with free bonding sites (dangling-H or dangling-O). The surface molecules and bonds of interest are identified for a simulated structurally relaxed 4-nm crystal in Fig. 6 (using the TIP4P potential).[79] The isotopic exchange most informative of the subject of this review is reflected in the FTIR spectroscopy of the dangling-D molecules. As discussed below, proton activity is signalled by lost of band intensity of the 2726 cm^{-1} band of the D_2O d-D bond and gain in intensity of the HDO d-D band at 2712 cm^{-1}. Because the d-D vibrations are largely localized on the "free" O-D bonds, the band frequencies are ~300 cm^{-1} above the interior O-D stretch bands. Thus, weak infrared bands of the surface molecules, used to

follow H-D exchange, can be viewed without interference from the interior ice bands.

As described previously, FTIR spectroscopy has been used to monitor isotopic exchange within[70] and on the surface of[21] ice nano-crystals in the 110-150 K temperature range. Helium aerosols of H_2O particles, with an average diameter in the 12 – 40 nm range, were prepared containing ~10% D_2O. As implied in Fig. 7, gas pulses from two separate one-liter He(g) reservoirs with the same total gas pressure, one containing 1.0% H_2O and the other ~0.1% D_2O, were transmitted via co-axial tubing to the inside of a double-walled cold-condensation cell. Simultaneous release and thorough overlap of the gas pulses allowed ice nanocrystals to form with nearly uniform distribution of D_2O between and within the particles. Some H-D exchange occurred during gas handling as well as during the cold-droplet phase of the nano-crystal formation process; but, as exemplified by the spectra in the right panel of Fig. 8, most of the deuterium usually appeared as intact isolated D_2O.

Isotopic exchange in the ice nanocrystal interior occurs on the time scale of hours to minutes in the 130 – 150 K range, much as observed for thick ice films.[66] On the surface, the relative rate is ~20 times faster. In the example of Fig. 8, for temperatures near 135 K, the surface exchange is ~60% complete in 6 min during which time period the interior exchange is only ~6%. The loss of d-D intensity at 2725 cm^{-1} corresponds to a D_2O surface half-life of 3 min. This result, typical of kinetic runs for numerous aerosols of "pure" bare ice nanocrystals, suggests a ratio of 23 for the respective rates. However, results for the temperature dependence of the surface exchange rates, point to an activation energy of 5 kcal/mol which can be contrasted with the value of 9.5 kcal/mol reported for H-D exchange within micron-thick ice films. Thus the ratio of rates, surface-to-interior, is expected to decrease with increasing temperature.

Influence of Surface Adsorbates on Interior and Surface Proton Activity

Additional FTIR isotopic exchange data that inter-relate the proton activity at the surface and in the interior of ice nanocrystals have been obtained using sub-monolayer (sub-ML) amounts of weak acid and base dopants.[21] The influence of ammonia as a surface adsorbate is particularly informative. As observed for the interior of thick ice films,[74] a trace of adsorbed ammonia thoroughly stops both the interior and the surface proton activity of nanocrystals at temperatures below 150 K. Surprisingly, increasing the coverage to ~10% of an ML restarts the interior activity but not that of the surface. By contrast, 20% ML of H_2S on bare ice enhances both surface and interior proton activity by a factor ~2.5, a magnitude similar to that produced by 2% of an ML of HBr. Further, H_2S added after a trace of ammonia restarts the interior proton activity, while 50% of an ML of HCl restarts the proton activity and raises it to a level much greater than that of pure bare ice. In essence, both the interior and the surface proton activity at a given temperature can be varied over orders of magnitude using sub-ML amounts of acid and base adsorbates.

Surface and Interior Proton Activity from RIS Studies of Isotopic Exchange in Ultra-thin Ice Films

Initial reactive-ion-scatter (RIS) studies of proton activity were directed to isotopic exchange between a thin film of compact amorphous D_2O ice on a metal substrate with a fractional coverage of H_2O.[71] For Cs^+ beam energies below 35eV, no H-D exchange was detected below 100 K, but low-energy Cs^+ pickup of HDO was obvious at 140 K, signalling the onset of surface proton activity. More complex related studies showed that surface H-D exchange was extensive at sub-minute times at 140 K, while the proton activity was greatly reduced only a layer or two into the surface. This led to the conclusion that the surface proton activity exceeded that of the interior ice by at least an order of magnitude. However, the RIS technique is only sensitive for the

outer molecular layers of a sample, so definitive conclusions were not reached regarding proton mobility/concentration within the interior amorphous ice.

It is noteworthy that each of the major RIS results for the amorphous-ice surface agree closely with the isotopic-exchange data for ice nanocrystals, for which the D_2O surface half-life increases from one minute at 140 K to over 200 minutes at 100K, and for which the surface exchange rate is more than an order of magnitude that of the interior. The inability to use ion scatter to qualitatively check for interior proton mobility was partially overcome in a later study showing that protons released by HCl buried in ice are able to move to the ice surface.[73] The conclusion based on that new approach is also consistent with the isotopic exchange data for ice nanocrystals, which clearly show interior proton mobility in crystalline ice.[21,70] However, the response to adsorbates of the interior proton activity of nanocrystals as described above demonstrates that protons can move from the surface of ice to the interior at low temperatures, contradictory to interpretations of both the RIS[71,73] and the soft-landed-proton data.[69] Computational results discussed above suggest that the activation barrier of the exchange process inside pure ice nanoparticles originates mostly from a combination of surface autoionization, and proton injection from the surface to the crystal interior. The barrier corresponding to proton hopping between crystal lattice sites appears to be low.[76]

Implications Regarding H^+ and OH^- Ion Distributions in Ice and Water

The tracking of H-D isotopic-exchange rates in amorphous (via RIS) and crystalline (via FTIR) ice show that the proton activity at the ice surface in the 120 – 145 K range is at least an order-of-magnitude greater than in the ice interior. Since proton mobility within disordered ice is apparently significantly less than for crystalline ice,[80] the greatly enhanced surface proton activity is attributed to a much greater concentration of protons at the disordered surface. (Surface disorder of ice nanocrystals

is discussed in detail in Ref. 52.)

Further, the H-D exchange rates for nanocrystals exposed to ammonia can be interpreted in terms of a preference of the hydroxide ion for subsurface or interior regions of the particles. A trace of ammonia on the ice particle surface stops all exchange, presumably because of a shift of the self-ionization equilibrium to favour hydroxide over hydronium ions. The hydroxide is a much inferior H-D exchange agent (i.e., a nearly immobile defect), so the suppressed H^+ concentration is observed as loss of exchange activity. However, a sufficiently high OH^- concentration can restart the H-D exchange despite the exceedingly low mobility. The remarkable and pertinent point is that the exchange restarts in the interior but not at the surface following adsorption of 10% ML ammonia. This suggests that, as indicated by the simulations, the OH^- does not favour the surface sites in the manner observed for the proton, but this is not entirely conclusive in the absence of relative mobility values for surface and interior OH^-.

VII. Charging of air bubbles and oil droplets in water

A different piece of information about charges at water interfaces is brought by zeta-potential measurements on air bubbles and oil droplets in water. As a matter of fact, charging of air bubbles in water has been repeatedly reported in the last 100 years or more and has been reviewed recently.[81,82] Depending on the conditions (purity of water, etc.) different or even no charging of air bubbles was observed but predominantly the water surface charged negatively. Recently, a negative value of zeta-potential of air bubbles in water of about -35 mV was obtained.[83]

Since 1990s, there has been a renewed interest in charging of water surfaces connected with electrophoretic mobility measurements of oil droplets in water.[84]

Negative charging of the oil-water interface observed in these experiments has been interpreted in terms of surface accumulation of OH^-. Analogous conclusions have been also derived from zeta-potential and titration experiments on oil emulsions in water, which also allowed quantifying the values of both the adsorbed and diffuse charge.[85,86] The former was estimated to correspond to a ~0.5 M concentration of hydroxide anions at the oil-water interface. The interfacial presence of OH^- was also assumed or postulated for interpretation of disjoining pressure measurements in thin aqueous films.[87,88]

VIII. Discussion and Conclusions

The present paper attempts at summarizing our present knowledge on autoionization at the surface of water. Admittedly, the current picture is not free of controversy. On one hand, molecular dynamics simulations and ab initio calculations provide a picture of an acidic water surface due to a preference of hydronium cations for the top-most layer, while hydroxide anions do not exhibit any strong surface propensity. This picture is supported by surface sensitive spectroscopic measurements, such as VSFG, SHG, on liquid water and IR and ion scattering at the amorphous surface of ice. On the other hand, zeta potential measurements on air bubbles and oil droplets in water and titration experiments for aqueous oil emulsions show mostly negative charging of the surface interpreted in terms of adsorbed hydroxide ions giving a basic surface.

While it is probably not possible to fully resolve this controversy yet, we can speculate about four possible situations:

i)Water surface is neither basic nor acidic. Either there are no ions at the surface as textbooks suggest or there is equal amount of hydronium and hydroxide. In either case, this would be in conflict with all calculations and experiments presented here.

ii)Water surface is basic. This would conflict molecular level calculations and experiments but would be in line with the present interpretation of most macroscopic measurements (zeta potential and titration).

iii)Water surface is acidic. Here the situation is opposite - this is in line with microscopic experiments and calculations but in conflict with macroscopic measurements - with the notable exception of surface tension data. These show at appreciable concentrations increase in surface tension with respect to pure water for inorganic bases (and salts) but decrease for strong acids,[89] which means in terms of the Gibbs adsorption isotherm[90] depletion of hydroxide but enhancement of hydronium in the interfacial layer.[6] Note that at very low (sub-milimolar) concentrations a decrease in surface tension has been observed for salts (the so called Ray-Jones effect[91]). The very existence of this effect is still under dispute and has been recently reinvestigated;[92] in any case no Ray-Jones effect has been observed in SHG measurements of aqueous NaOH or KOH.[93]

iv) Water surface is both basic and acidic. This looks like a clear nonsense, unless different definitions of the surface are employed by the two groups. After all, the surface neutrality condition requires that on the whole the interfacial layer must be neutral (since the bulk is neutral, otherwise there would be neutralization currents). This implies that if the top layer is acidic due to accumulation of hydronium then the subsurface is basic thanks to increase concentration of hydroxide (and *vice versa*). The

thickness of this interfacial layer is concentration dependent and for low ion concentrations can extend to many water layers. Simulations and surface selective spectroscopies of both neat water, as well as acid and base solutions of varying concentrations, probe preferentially the topmost layer or at most few additional subsurface layers. It may be hard to fully specify to what surface thickness the zeta potential and titration experiments refer, but probably it is significantly larger. It would be tempting to reconcile the two views in this way but we do not hide from the reader that the basic problem of the polarity of the top layer would probably not be fully resolved. Clearly, more sophisticated experiments and advanced simulations are needed in the future to resolve this issue, which has possible implications for reactivity at environmentally or technologically relevant aqueous surfaces.

Acknowledgement

Support from the Czech Ministry of Education (grants LC512 and ME644), the Granting Agency of the Czech Republic (grant 202/06/0286), and the US-NSF (grants CHE 0431312 and 0209719) is gratefully acknowledged by PJ. LV acknowledges support from the Granting Agency of the Czech Republic (grant 203/05/H001), VB and JPD acknowledge the funding of the Israel-US Binational Science Foundation. AM thanks the Centers CECIC-CIMENT and IDRIS for providing computer facilities.

References

[1] L. Onsager, N. N. T. Samaras, *J. Chem. Phys.,* 1934, **2,** 528.

[2] J. E. B. Randles, *Phys. Chem. Liq.,* 1977, **7,** 107.

[3] P. Jungwirth, D. J. Tobias, *J. Phys. Chem. B,* 2001**, 105***,* 10468.

[4] L. X. Dang, T.-M. Chang, *J. Phys. Chem. B,* 2002, **106***,* 235.

[5] T.-M. Chang, L. X. Dang, *Chem. Rev.,* 2006, **106***,* 1305.

[6] P. Jungwirth, D. J. Tobias, *Chem. Rev.,* 2006, **106***,* 1259.

[7] G. Archontis, E. Leontidis, G. Andreou, *J. Phys. Chem. B,* 2005**, 109***,* 17957.

[8] D. Liu, G. Ma, L. M. Levering, H. C. Allen, *J. Phys. Chem. B,* 2004**, 108***,* 2252.

[9] E. A. Raymond, G. L. Richmond, *J. Phys. Chem. B,* 2004**, 108***,* 5051.

[10] S. Gopalakrishnan, D. Liu, H. C. Allen, M. Kuo, M. J. Shultz, *Chem. Rev.,* 2006, **106***,* 1155.

[11] P. B. Petersen, R. J. Saykally, *Annu. Rev. Phys. Chem.,* 2006, **57***,* 333.

[12] B. Winter, M. Faubel, *Chem. Rev.,* 2006, **106***,* 1176.

[13] P. B. Petersen, R. J. Saykally, *J. Phys. Chem. B,* 2005**, 109***,* 7976.

[14] T. L. Tarbuck, S. T. Ota, G. L. Richmond, *J. Am. Chem. Soc.,* 2006**, 128***,* 14519.

[15] L. X. Dang, *J. Chem. Phys.,* 2003, **119***,* 6351.

[16] M. K. Petersen, S. S. Iyengar, T. J. F. Day, G. A. Voth, *J. Phys. Chem. B,* 2004**,** **108***,* 14804.

[17] J. W. Shin, N. I. Hammer, E. G. Diken, M. A. Johnson, R. S. Walters, T. D. Jaeger, M. A. Duncan, R. A. Christie, K. D. Jordan, *Science,* 2004, **304***,* 1137.

[18] M. Miyazaki, A. Fujii, T. Ebata, N. Mikami*, Scienc*e 2004, **304**, 1134.

[19] S. S. Iyengar, T. J. F. Day, G. A. Voth, *Int. J. Mass Spectr.,* 2005**, 241***,* 197.

[20] M. Mucha, T. Frigato, L. M. Levering, H. C. Allen, D. J. Tobias, L. X. Dang, P. Jungwirth, *J. Phys. Chem. B,* 2005**, 109***,* 7617.

[21] V. Buch, A. Milet, R. Vacha, P. Jungwirth, J. P. Devlin, *Proc. Nat. Acad. Sci. USA, in press.*

[22] H. W. Gilbert, P. E. Shaw, *Proc. Phys. Soc. London,* 1924, **37***,* 195.

[23] A. Graciaa, G. Morel, P. Saulner, J. Lachaise, R. S. Schechter, *J. Colloid Interface Sci.,* 1995, **172***,* 131.

[24] K. G. Marinova, R. G. Alargova, N. D. Denkov, O. D. Velev, D. N. Petsev, I. B. Ivanov, R. P. Borwankar, *Langmuir,* 1996, **12***,* 2045.

[25] J. K. Beattie, A. M. Djerdjev, *Angew. Chem. Int. Ed.,* 2004, **43***,* 3568.

[26] J. K. Beattie, *Lab Chip,* 2006, **6***,* 1409.

[27] J. K. Beattie, *in: Colloid Stability: The Role of Surface Forces, Part II,* ed. T. F.

Tadros, Wiley, Weinheim, 2006, p. 153.

[28] K. A. Karraker, C. J. Radke, *Adv. Colloid Interface Sci.,* 2002, **96***,* 231.

[29] G. Andaloro, M. A. Palazzo, M. Migliore, S. L. Fornili, *Chem. Phys. Lett.,* 1988, **149***,* 201.

[30] S. L. Fornili, M. Migliore, M. A. Palazzo, *Chem. Phys. Lett.,* 1986, **125***,* 419.

[31] E. Brodskaya, A. P. Lyubartsev, A. Laaksonen, *J. Phys. Chem. B,* 2002**, 106***,* 6479.

[32] J.-L. Kuo, M. L. Klein, *J. Chem. Phys.,* 2005**, 122***,* 024516.

[33] A. Vegiri, S. V. Shevkunov, *J. Chem. Phys.,* 2000**, 113***,* 8521.

[34] M. Zapalowski, W. M. Bartczak, *Comp. Chem.,* 2000**, 24***,* 459.

[35] E. Lindhal, B. Hess, D. van der Spoel, *J Mol Model.*, 2001, **7**, 306.

[36] T. Kubar, M. Hanus, F. Ryjacek, P. Hobza, *Chem. Eur. J.* 2006, **12**, 280.

[37] J. W. Caldwell, P. A. Kollman, *J. Phys. Chem.* 1995, **99,** 6208.

[38] C. I. Bayly, P. Cieplak, W. D. Cornell, P. A. Kollman, P. A., *J. Phys. Chem.* 1993, ***97***, 10269.

[39] L. Perera, U. Essmann, M. L. Berkowitz, *J. Chem. Phys.* 1995, **102,** 450.

[40] A. Warshel, R. M. Weiss, *J. Am. Chem. Soc.* 1980, **102**, 6218.

[41] M. A. Lill, V. Helms, *J. Chem. Phys.* 2001, **115**, 7993.

[42] S. S. Iyengar, M. K. Petersen, T. J. F. Day, C. J. Burnham, V. E. Teige, G. A. Voth, *J. Chem. Phys.* 2005, **123**, 084309.

[43] C. J. Burnham, M. K. Petersen, T. J. F. Day, S. S. Iyengar, G. A. Voth, *J. Chem.*

Phys. 2006, **124**, 024327.

[44] P. L. Geissler, C. Dellago, D. Chandler, J. Hutter, M. Parrinello, *Science* 2001, **292**, 2121.

[45] J. VandeVondele, M. Krack, F. Mohamed, M. Parrinello, T. Chassaing, J. Hutter, *Computer. Phys. Comm.* 2005, **167**, 103.

[46] S. Goedecker, M. Teter, J. Hutter, *J. Phys. Rev. B*, 1996, **54**, 1703.

[47] I. W. Kuo, C. J. Mundy, *Science*, 2004, **303**, 658.

[48] G. J, Martyna, M. E. Tuckerman, *J. Chem. Phys.* 1999, **110**, 2810

[49] A. J, Easteal, W. E. Price, L. A. Woolf, *J. Chem. Soc., Faraday Trans*. I, 1989, **85**, 1091.

[50] M. Holz, S. R. Heil, A. Sacco, *Phys. Chem. Chem. Phys*. 2000, **2**, 4740.

[51] D. Svozil, P. Jungwirth, *J. Phys. Chem. A* 2006, **110**, 9194.

[52] V. Buch, S. Bauerecker, J. P. Devlin, U. Buck, J. K. Kazimirski, *Int. Rev. Phys. Chem*. 2004, **23**, 375.

[53] V. Buch, R. Martonak, M. Parrinello, *J. Chem. Phys*. 2006, **124**, 204705.

[54] W. L. Jorgensen, J. D. Madura, *Mol. Phys.* 1985, **56**, 1381.

[55] M. E. Tuckerman, A. Chandra, D. Marx, *Acc. Chem. Res.* 2006, **39**, 151.

[56] H. Groenzin, I. Li, M. J. Shultz, to appear in Proceedings of 111 Conference on Physics and Chemistry of Ice (2007).

[57] A. Glebov, A. P. Graham, A. Menzel, J. P. Toennies, P. Senet, *J. Chem. Phys*. 2000, **112**, 11011.

[58] P.V. Hobbs, *Ice Physics*, Clarendon, Oxford, 1974.

[59] V.F. Petrenko, R. W. Whitworth, *Physics of Ice*, Oxford Univ. Press, Oxford, 1999.

[60] V. Buch, P. Sandler, J. Sadlej, *J. Phys. Chem. B* 1998, **102**, 8641.

[61] S. McDonald, L. Ojamae, S. J. Singer, *J. Phys. Chem. A* 1998, **102**, 2824.

[62] J. L. Kuo, J. V. Coe, S. J. Singer, Y. B. Band, L. Ojamae, *J. Chem. Phys.* 2001, **114**, 2527.

[63] Q. Du, R. Superfine, E. Freysz, Y. R. Shen, *Phys. Rev. Lett.* 1993, **70,** 2313.

[64] H. C. Allen, E. A. Raymond, G. L. Richmond, *J. Phys. Chem. A* 2001, **105,** 5313.

[65] A. Von Hipple, D. B. Knoll, W. B. Westphal, *J. Chem. Phys.* 1971, **54**, 134.

[66] W. B. Collier, G. Ritzhaupt, J. P. Devlin, *J. Phys. Chem*. 1984, **88**, 363.

[67] P. J. Wooldridge, J. P. Devlin*, J. Chem. Phys*. 1988, **88**, 3086.

[68] J. P. Devlin, *J. Phys. Chem*. 1988, **92**, 6867.

[69] J. P. Cowin, A. A. Tsekouras, M. J. Iedema, K. Wu, G. B. Ellison, *Nature* 1999, **398**, 405.

[70] N. Uras-Aytemiz, C. Joyce, J. P. Devlin, *J. Chem. Phys*. 2001, **115**, 9835.

[71] S. C. Park, K-H. Jung, H. Kang, *J. Chem. Phys.* 2004, **121**, 2765.

[72] H. Kang, *Acc. Chem. Res*. 2005, **38**, 893.

[73] C-W. Lee, P-R. Lee, H. Kang, *Angew. Chem*. 2006, **118**, 5655.

[74] J. P. Devlin, in *Proton Transfer in Hydrogen-Bonded Systems*, ed. T. Bountis, NATO ASI Series, Plenum Press, New York, 1992, Vol. 291, pp 249 – 260.

[75] N. Grishina, V. Buch, *J. Chem. Phys*. 2004, **120**, 5217.

[76] C. Kobayashi, S. Saito, I. Ohmine, *J. Chem. Phys.* 2000, **113**, 9090.

[77] J. P. Devlin, *Int. Rev. Phys. Chem*. 1990, **9**, 29.

[78] M. Kunst, J. M. Warman, *J. Phys. Chem.* 1983, **83**, 4093.

[79] J. P. Devlin, C. Joyce, V. Buch, *J. Phys. Chem. A* 2000, **104**, 1974.

[80] M. Fisher, J. P. Devlin, *J. Phys. Chem.* 1995, **99**, 11584.

[81] A. Graciaa, P. Creux, J. Lachaise, in *Electrokinetics of Bubbles*, ed. A. T. Hubbard, Dekker, New York, 2002.

[82] A. Graciaa, P. Creux, J. Lachaise, *Surf. Sci. Ser*., 2002, **106**, 825.

[83] M. Takahashi, *J. Phys. Chem. B*, 2005, **109**, 21858.

[84] K. G. Marinova, R. G. Alargova, N. D. Denkov, O. D. Velev, D. N. Petsev, I. B. Ivanov, R. P. Borwankar, *Langmuir*, 1996, **12**, 2045.

[85] J. K. Beattie, A. M. Djerdjev, A. M., *Angew. Chem. Int. Ed.* 2004, **43**, 3568.

[86] J. K. Beattie, *Lab Chip* 2006, **6**, 1409.

[87] K. A. Karraker, C. J. Radke, *Adv. Colloid Interface Sci.* 2002, **96,** 231.

[88] R. von Klitzing, C. Stubenrauch, *J. Phys. Condens. Matter* 2003, **15,** R1197.

[89] P. K. Weissenborn, R. J. Pugh, *J. Colloid Interface Sci*. 1996, **184**, 550.

[90] J. W. Gibbs, *The Collected Works of J. Willard Gibbs*, Longmans, New York, 1928.

[91] G. Jones, W. A. Ray, *J. Am. Chem. Soc.* 1937, **59,** 187.

[91] P. B. Peterson, R. J. Saykally, *J. Am. Chem. Soc.* 2005, **127**, 15446.

[92] P. B. Petersen, R. J. Saykally, *in preparation*.

Table 1: Charges (e), polarizabilities (α) in $Å^3$, and Lennard-Jones parameters in

Gromacs convention (σ in Å and ε in kJ/mol) for the investigated ions. O-H bonds were constrained to 0.98 Å for H_3O^+, 0.98 and 1.20 Å for the side and central H-atoms of $H_5O_2^+$, and 1.00 Å for OH^-. The correct pyramidal shape and bond angles of H_3O^+ were secured by constraining the H-H distances to 1.63 Å. For $H_5O_2^+$, for the central hydrogen the O-H-O and H-O-H angles were constrained to 173° and 118°, while for the side hydrogens the H-O-H angle was fixed to 109°. The H-O-O-H dihedral potential has a minimum of 0.837 kJ/mol at 90°.

	e	**α**	σ	**ε**
O (H_3O^+)	-0.4166	0.98	3.050	0.617
H (H_3O^+)	+0.4722	0.0	0.0	0.0
O ($H_5O_2^+$)	-0.5900	1.19	3.204	0.652
H (central, $H_5O_2^+$)	+0.3800	0.0	0.0	0.0
H (side, $H_5O_2^+$)	+0.4500	0.0	0.0	0.0
O (OH^-)	-1.3500	2.00	3.840	0.626
H (OH^-)	+0.3500	0.0	0.0	0.0

Figure captions

Fig. 1: A characteristic snapshot of a water slab with a single hydronium at the surface and a hydroxide ion in the bulk

Fig. 2: Profiles of potential energies corresponding to NVT (at 270 K) on-the-fly trajectories of Zwitterionic systems containing an H_3O^+/OH^- ion pair (black), and of corresponding neutral liquid H_2O systems without ions (red). (A) A ~11 A thick slab of water in a two-dimensional periodic box. (B) A cubic box of water, with 3D periodic boundaries. (Arrows mark the time of the ion-pair recombination.)

Fig. 3: Favorable surface sites for the hydronium (A, blue) and the hydroxide (B, yellow) in the ice basal plane surface. Only the top ice bilayer is shown. The water molecules which are near-neighbors to the ions are four-coordinated, with one H-bond to the second bilayer. The second near-neighbor molecules, marked by circles, are three coordinated, with either a d-H atom (dashed circle) or d-O (dotted).

Fig. 4: Motion and energy profile of proton and hydroxide in ice during energy minimization. Two simulation cells are shown, since recombination occurred across periodic boundary. Sites visited by the hydroxide in the course of the minimization are marked yellow. Sites visited by the hydronium are marked blue. The inset shows energy as a function of a minimization step. The letters in the inset correspond to proton jump events noted in molecular graphics. The arrow denotes proton jump corresponding to ion recombination.

Fig. 5: Panels showing the presence of a proton (H_3O^+) and orientational L defect within an ice segment, and the effect on an isolated D_2O molecule from passage of the

proton (middle panel) and the L defect (bottom panel).

Fig. 6: Stick model of a simulated structurally relaxed 4 nm ice crystal obtained using a TIP4P potential. The bilayer-thick cross section shows clearly the ordered crystalline core and disordered surface with dangling bonds of surface molecules.

Fig. 7: Infrared cold-condensation cell and associated manifold for the preparation of ice nanocrystals containing isolated D_2O, and for the FTIR monitoring of isotopic exchange within and at the surface of the ice particles.

Fig. 8: Sequential FTIR spectra showing the conversion of isolated D_2O molecules to HDO for the surface (left panel: from the bottom) and the interior (right panel) of an aerosol of ice nanocrystals during 6 min at 135 K. Arrows at right indicate decreasing D_2O and increasing HDO content with time.

Figure 1:

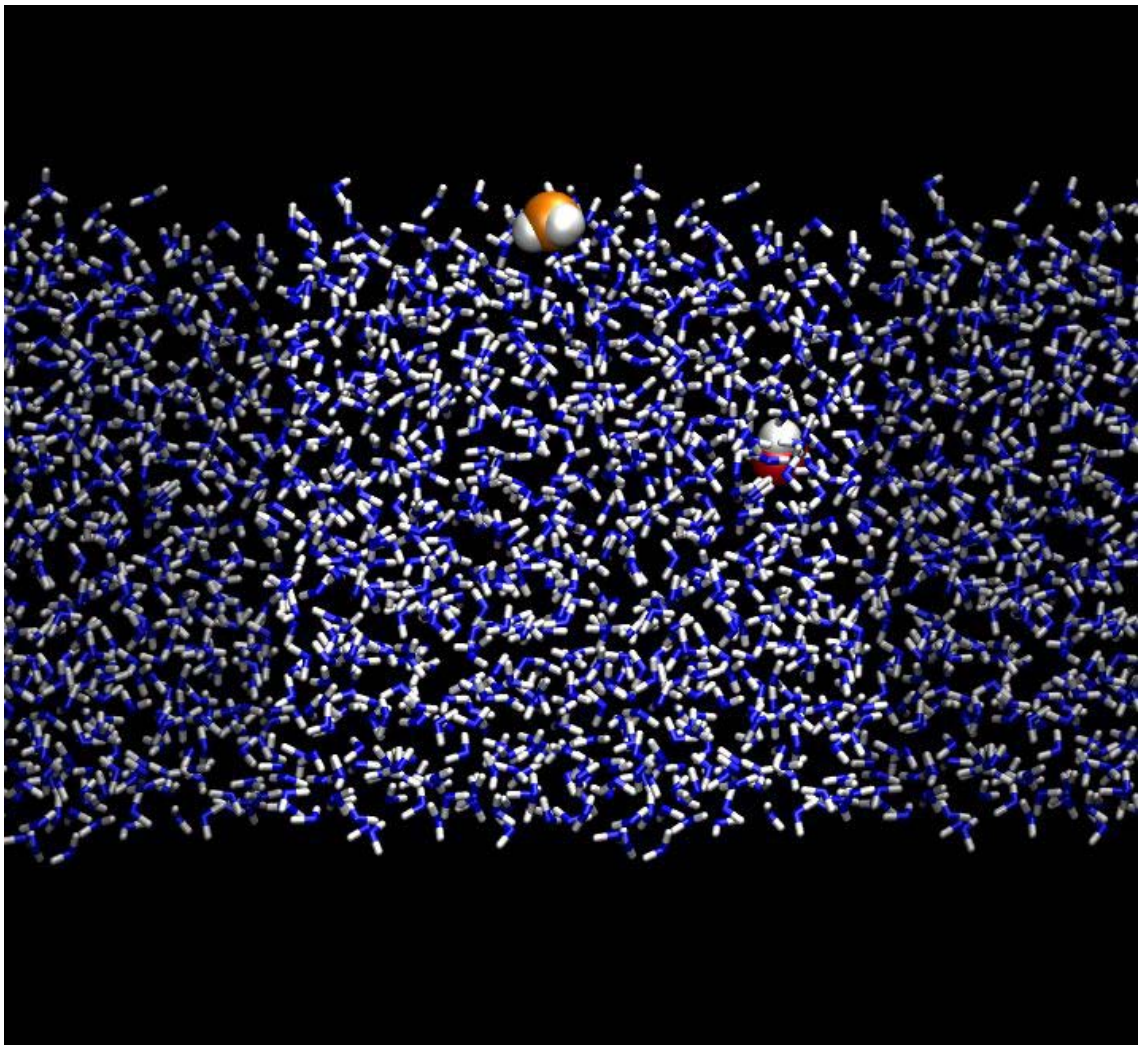

Fig. 2:

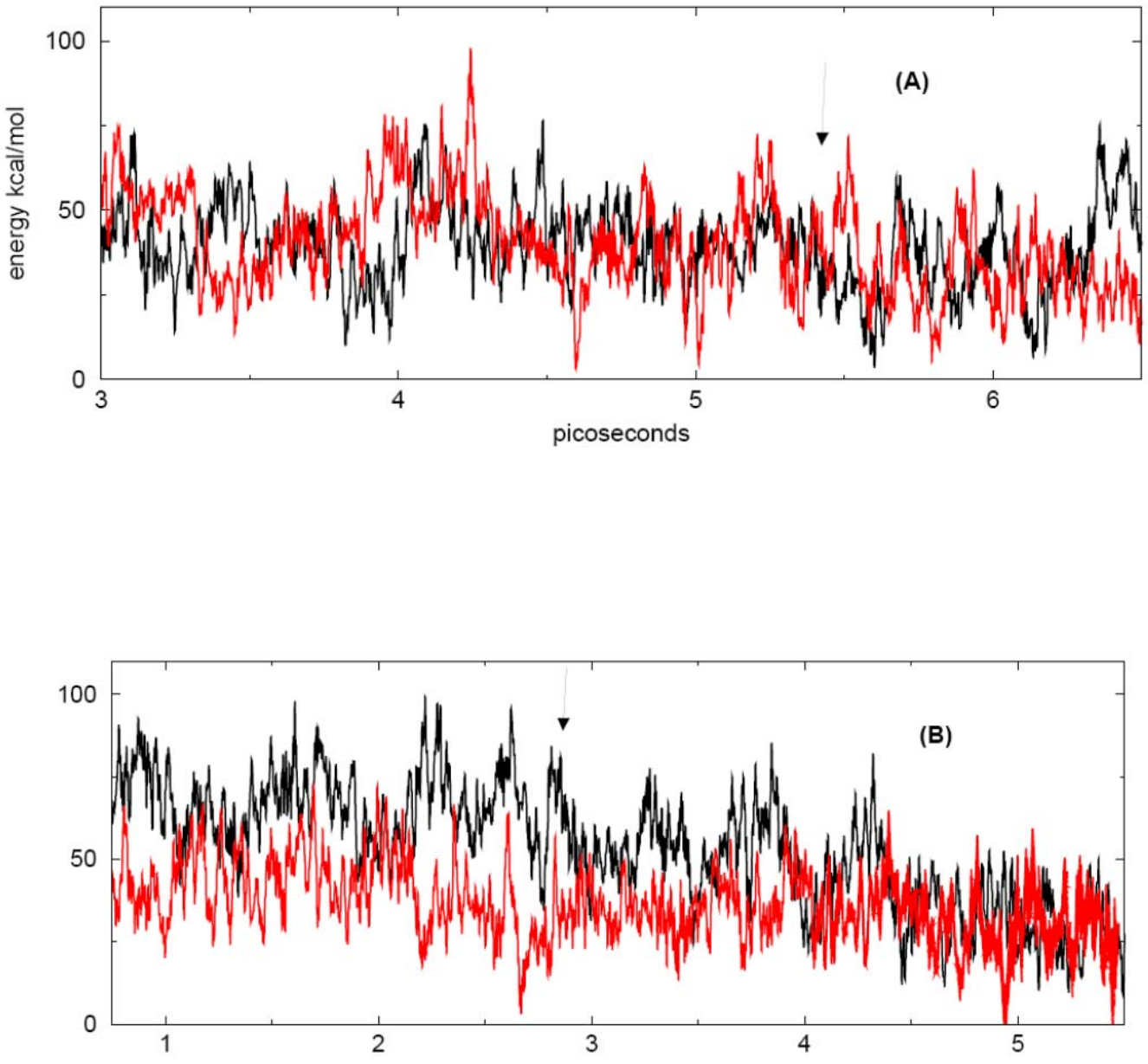

Fig. 3:

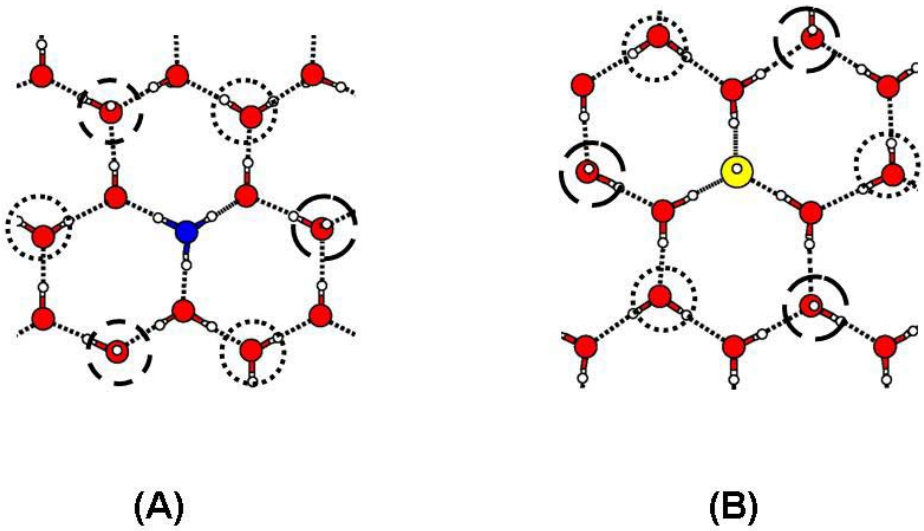

(A) (B)

Fig. 4:

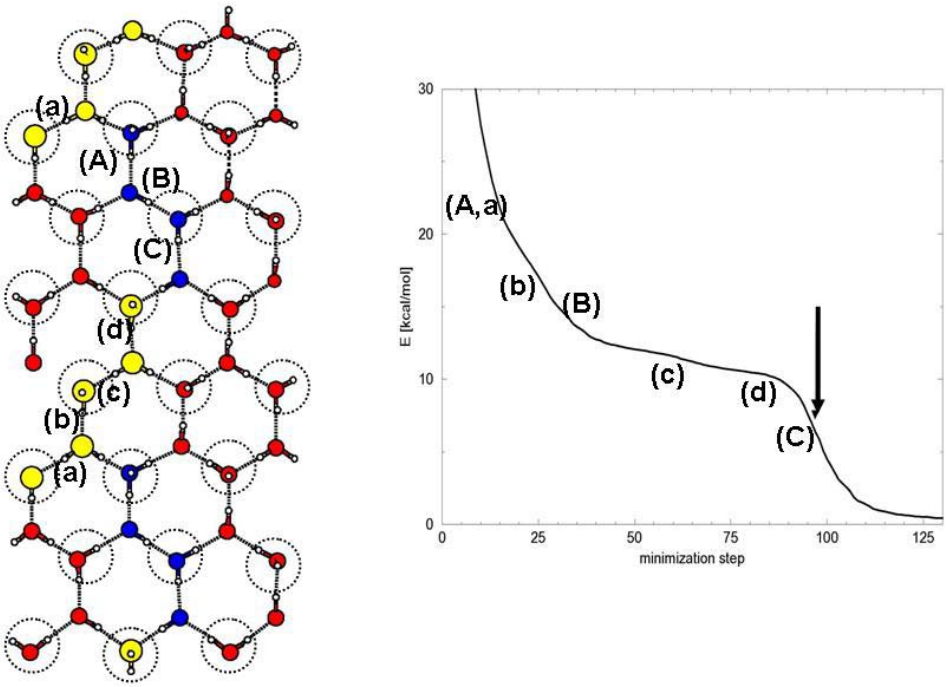
(a)
(A)
(B)
(C)
(d)
(c)
(b)
(a)
30
20
10
0
E [kcal/mol]
(A,a)
(b)
(B)
(c)
(d)
(C)
0
25
50
75
100
125
minimization step

Fig. 5:

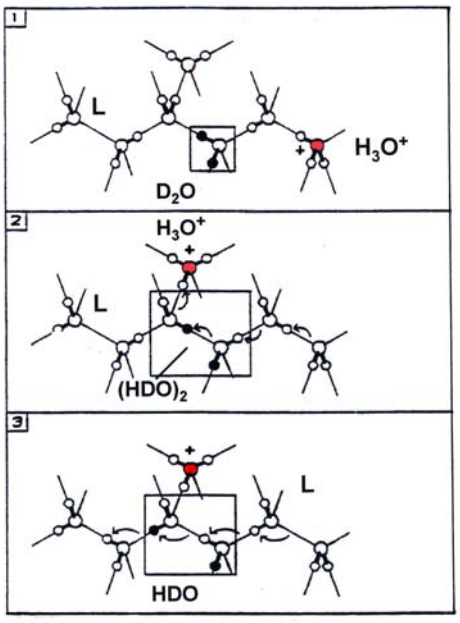

Fig. 6:

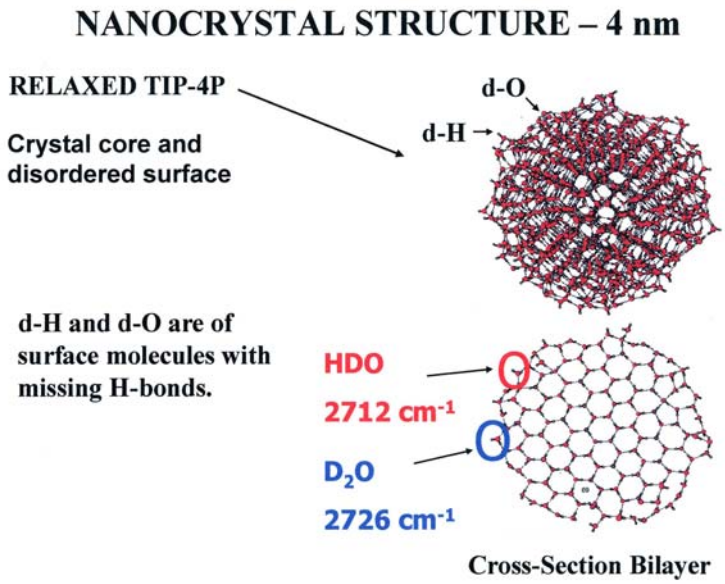
NANOCRYSTAL STRUCTURE – 4 nm
RELAXED TIP-4P
Crystal core and disordered surface
d-O
d-H
d-H and d-O are of surface molecules with missing H-bonds.
HDO
2712 cm-1
D2O
2726 cm-1
Cross-Section Bilayer

Fig. 7:

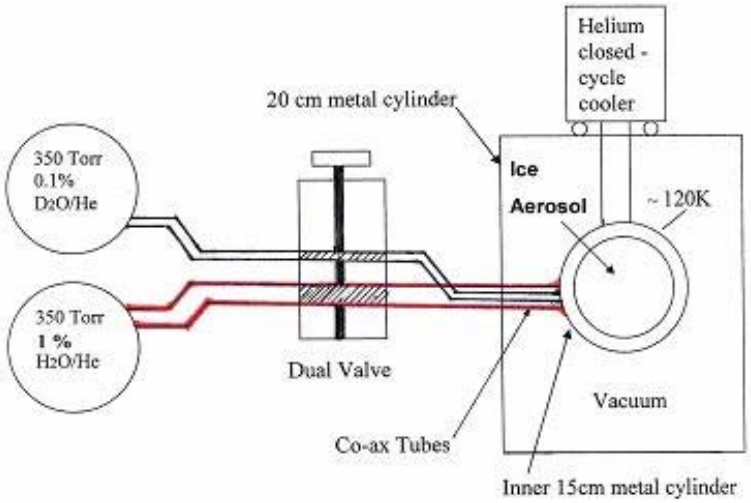
Helium
closed -
cycle
cooler
20 cm metal cylinder
Ice
Aerosol
~ 120K
350 Torr
0.1%
D2O/He
350 Torr
1 %
H2O/He
Dual Valve
Vacuum
Co-ax Tubes
Inner 15cm metal cylinder

Fig. 8:

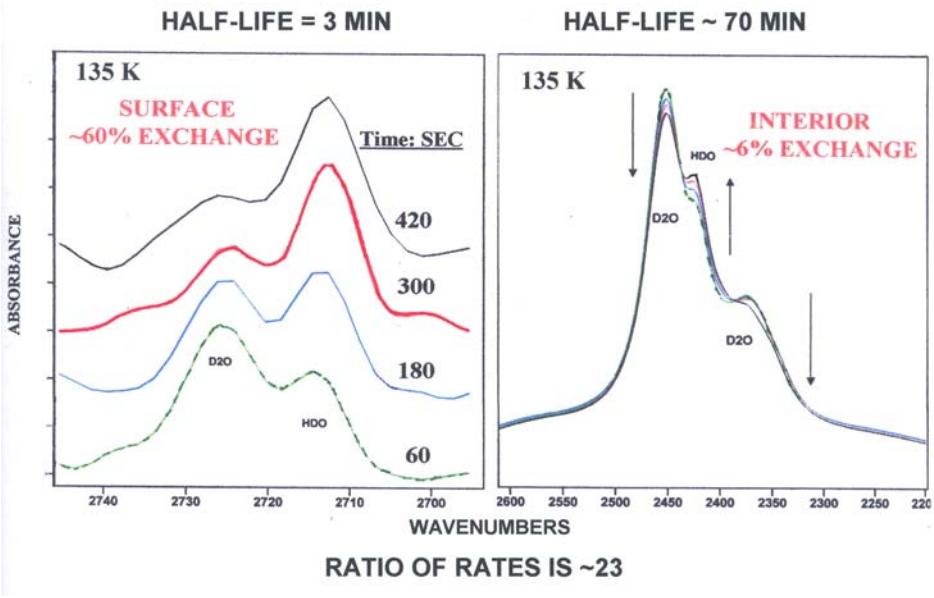
HALF-LIFE = 3 MIN
HALF-LIFE ~ 70 MIN
135 K
SURFACE
~60% EXCHANGE
Time: SEC
420
300
180
60
D2O
HDO
135 K
INTERIOR
~6% EXCHANGE
HDO
D2O
D2O
ABSORBANCE
2740
2730
2720
2710
2700
2600
2550
2500
2450
2400
2350
2300
2250
WAVENUMBERS
RATIO OF RATES IS ~23